



# Synthesis of magnetite using petai (*Parkia speciosa*) peel extract with ultrasonic waves as reusable catalysts for biodiesel production from waste frying oil

Maya Rahmayanti <sup>a,\*</sup>, Annisa Nurul Syakina <sup>a</sup>, Triastuti Sulistyanyingsih <sup>b</sup>, Budi Hastuti <sup>c</sup>

<sup>a</sup> Department of Chemistry, Faculty of Science and Technology, Universitas Islam Negeri Sunan Kalijaga, Yogyakarta, Indonesia

<sup>b</sup> Department of Chemistry, Universitas Negeri Semarang, Semarang, Indonesia

<sup>c</sup> Department of Chemistry Education, Faculty of Teacher Training and Education, Sebelas Maret University, Surakarta, Central Java, Indonesia

\* Corresponding author: [maya.rahmayanti@uin-suka.ac.id](mailto:maya.rahmayanti@uin-suka.ac.id)

<https://doi.org/10.14710/jksa.26.4.125-132>

## Article Info

### Article history:

Received: 21<sup>st</sup> December 2022

Revised: 25<sup>th</sup> May 2023

Accepted: 29<sup>th</sup> May 2023

Online: 30<sup>th</sup> June 2023

### Keywords:

biodiesel; magnetite;  
 sonochemistry; waste frying oil;  
 reusable catalysts

## Abstract

Magnetite synthesis using petai (*Parkia speciosa*) peel extract using the sonochemical method ( $\text{Fe}_3\text{O}_4$ -PPE) has been successfully carried out.  $\text{Fe}_3\text{O}_4$ -PPE is applied as a catalyst in biodiesel production. This study aimed to determine the physical and chemical characteristics of  $\text{Fe}_3\text{O}_4$ -PPE and its ability as a reusable catalyst in biodiesel production using waste frying oil as the primary raw material. Characterization of  $\text{Fe}_3\text{O}_4$ -PPE was carried out using FTIR, XRD, and PSA instruments. Biodiesel was produced in 3 reaction cycles with the same  $\text{Fe}_3\text{O}_4$ -PPE catalyst. The results of the FTIR characterization showed that the  $\text{Fe}_3\text{O}_4$ -PPE catalyst had Fe-O bonds from  $\text{Fe}_3\text{O}_4$  and -OH phenolic groups, -C-O, -C=C aromatic compounds derived from petai peel extract. The crystal size of the  $\text{Fe}_3\text{O}_4$ -PPE catalyst based on the results of calculations using Debye-Scherrer from the XRD chromatogram is 9.41 nm. The particle size of the  $\text{Fe}_3\text{O}_4$ -PPE catalyst based on analysis using PSA was divided into three groups, namely, 5.4 nm, 195 nm, and 2702.6 nm.  $\text{Fe}_3\text{O}_4$ -PPE was successfully used as a reusable catalyst for three cycles of biodiesel production using waste frying oil as raw material. The characteristics of  $\text{Fe}_3\text{O}_4$ -PPE before and after being used as a catalyst did not change. Based on GC-MS analysis, the fatty acid methyl ester (FAME) composition of biodiesel is palmitic acid and oleic acid.

## 1. Introduction

Research on renewable energy sources has received severe attention recently due to the increasing global demand. At the same time, fossil fuels are limited and can pollute the environment [1]. One of the most developed renewable energy is biodiesel. Biodiesel is also green fuel containing fatty acid methyl ester (FAME). Biodiesel is synthesized through the trans-esterification reaction of triglyceride oils, such as non-edible or edible vegetable oils, with alcohol using a catalyst.

The advantages of biodiesel compared to fossil fuels are that it is non-toxic, comes from renewable resources, emits fewer air pollutants, has a high cetane number, and is free of sulfur compounds [1, 2]. The main drawback of

biodiesel production is the high cost of raw materials. Today's primary raw materials are vegetable (edible) oils, such as soybean and palm. It can disrupt food security, especially in low-income and developing countries [1]. The solution is to seek innovative development of raw materials that do not interfere with food security and are environmentally friendly is exciting research to develop.

In this research, the raw material used is waste frying oil, a household waste that can cause environmental pollution. Used waste frying oil contains triglycerides (TG) and free fatty acids (FFA), which can be reacted with an alcohol to produce methyl esters (biodiesel). The challenge is that the FFA content in used waste frying oil is higher than the (TG) content, so selecting a suitable catalyst is very important to study.

Conventionally, the catalysts that are widely used are homogeneous catalysts such as NaOH and H<sub>2</sub>SO<sub>4</sub> [3, 4]. This type of catalyst can produce biodiesel with a high yield and reaction rate but produces a large volume of wastewater [5]; it can cause soap to form when it reacts with FFA, so the separation process will be complicated and cause production costs to increase. It is difficult to reuse [6]. Enzymatic catalysts have also begun to be widely developed but require high costs and low reaction rates [7].

Heterogeneous catalysts are the right choice to replace homogeneous and enzymatic catalysts [8, 9]. This catalyst is insoluble in alcohol, so that it can be easily separated [1]. In addition, this catalyst can be easily reused (reusable). However, most heterogeneous catalysts require reusing filtration and centrifugation processes, which has an impact on increasing operating time, energy consumption, and production costs. This problem can be overcome by separating a heterogeneous catalyst as a magnetic catalyst using an external magnetic field and reused [10]. Magnetic catalysts can also be used in mass production with relatively low production costs [11, 12].

This research made a magnetic catalyst based on a petai (*Parkia speciosa*) peel modified with magnetite (Fe<sub>3</sub>O<sub>4</sub>) using the sonochemical method and used to produce biodiesel from used waste frying oil as raw material. Petai peel contains phenolic compounds with abundant hydroxy groups [13, 14, 15, 16], which can be heterogeneous catalysts in the (TG)/FFA reaction with alcohol. Magnetite is an iron oxide compound with superparamagnetic properties [17, 18, 19, 20], making the catalyst separation process at the end of the reaction easier. It can be used repeatedly in subsequent synthesis processes. The novelty of this research is the synthesis method that uses the sonochemical method and its application as a reusable catalyst in biodiesel synthesis.

## 2. Materials and Methods

### 2.1. Equipment and Materials

The equipment used in this study was a set of glassware, a hot plate, and an external magnetic field. The waste frying oil and petai peel used were obtained from household waste. Chemicals such as methanol (CH<sub>3</sub>OH), iron (III) chloride (FeCl<sub>3</sub>·6H<sub>2</sub>O), iron (II) sulfate (FeSO<sub>4</sub>·7H<sub>2</sub>O), sodium hydroxide (NaOH), sulfuric acid (H<sub>2</sub>SO<sub>4</sub>), 95% ethanol, and phenolphthalein indicator were of analytical grade and purchased from Merck. Distilled water with two times distillation was used as a solvent.

### 2.2. Extraction of Petai Peel

Petai peel was washed with water and dried in the sun for 15 days to remove moisture. Furthermore, the dried petai peel was cut into small pieces and blended. Twenty grams of petai peel powder were transferred to an erlenmeyer containing 200 mL of double-distilled water and boiled for 20 minutes at 60°C. Then, the resulting extract was filtered using Whatman No. 1 filter paper, and the filtrate was stored at 4°C for further use.

### 2.3. Sonochemical Synthesis of Magnetite using Petai (*Parkia speciosa*) Peel Extract

Magnetite from petai peel extract (Fe<sub>3</sub>O<sub>4</sub>-PPE) was synthesized using the sonochemical method by providing a flow of ultrasonic waves with a frequency of 800 kHz. As much as 1.082 g FeCl<sub>3</sub>·6H<sub>2</sub>O/50 mL double-distilled water was mixed with 0.556 g FeSO<sub>4</sub>·7H<sub>2</sub>O/50 mL double-distilled water. A mixture of Fe<sup>3+</sup> and Fe<sup>2+</sup> solutions was added to 1 M NaOH solution before 15 mL of petai peel extract was added. The pH of the mixture was measured, then stirred for 60 minutes at 60°C with constant stirring. The pH of the mixture was remeasured. The black precipitate obtained was decanted using an external magnetic field, then washed with double-distilled water two times. The precipitate was dried in an oven at 100°C for 3 hours. The dried precipitate was weighed, and the yield was measured.

### 2.4. Characterization of Fe<sub>3</sub>O<sub>4</sub>-PPE

Fe<sub>3</sub>O<sub>4</sub>-PPE's functional groups were characterized using a Fourier transform infrared spectroscopy (FTIR, Shimadzu Prestige 21), and the crystal size and crystallinity of Fe<sub>3</sub>O<sub>4</sub>-PPE were determined using X-ray diffraction (XRD, XRD-6000 Shimadzu). The particle size was analyzed using a particle size analyzer (PSA, Horiba SZ-100).

### 2.5. Pre-treatment of Waste Frying Oil Through the Filtration Method

A 300 mL waste frying oil (WFO) was filtered using Whatman No. 1 filter paper at room temperature to separate solid impurities. The filtered WFO was tested for free fatty acid content.

### 2.6. Determination of Free Fatty Acid Content from Waste Frying Oil

Two grams of WFO were dissolved in 50 mL of 95% ethanol. Then five drops of phenolphthalein indicator were added and stirred for 30 seconds. The titration using 0.1 N NaOH solution was stopped when the color of the solution turned pink for about 30 seconds. The volume of NaOH used to change the color of the solution was recorded. %FFA of WFO was calculated using Equation (1).

$$\%FFA = \frac{V_{NaOH} \times N_{NaOH} \times \text{fatty acid molecular weight} \times 100}{\text{Weight of WFO (mg)}} \quad (1)$$

### 2.7. Biodiesel Production

#### 2.7.1. Esterification Reaction of WFO

The esterification reaction was performed using a batch reactor. WFO and methanol were mixed in a ratio of 1:10, and a Fe<sub>3</sub>O<sub>4</sub>-PPE catalyst was added with various concentrations of 5% and 10% by weight of the WFO. The mixture was stirred for 60 minutes at 60°C. The reaction mixture was put into a separatory funnel and allowed to stand for 5 hours until two layers were formed. The bottom layer was a mixture of catalyst and water, while the top layer was a mixture of biodiesel, triglycerides, and residual methanol. Furthermore, the top layer was used for the transesterification reaction step. The catalyst in the lower layer was recovered using an external magnetic field.

### 2.7.2. Transesterification Reaction of WFO

The top layer resulting from the esterification reaction was added with methanol and  $\text{Fe}_3\text{O}_4$ -PPE catalyst with the ratio of the top mixture: methanol of 1:5 and 5% of the top mixture by weight of the top mixture. The mixture was stirred for 60 minutes at 60°C. The reaction mixture was put into a separatory funnel and allowed to stand for 5 hours until two layers were formed. The bottom layer was a mixture of catalyst and glycerol, while the top layer was a mixture of biodiesel and residual methanol. The above mixture was distilled at 60°C to evaporate the methanol.

### 2.7.3. Reusability of $\text{Fe}_3\text{O}_4$ -PPE Catalyst

Biodiesel production was conducted for three cycles using the same catalyst. The  $\text{Fe}_3\text{O}_4$ -PPE catalyst was recovered using an external magnetic field in each reaction cycle. Then, the catalyst was rinsed thoroughly with acetone to remove any organic species adhering to the catalyst's surface. After drying at 100°C for 12 hours, the catalyst obtained was reused for the next biodiesel production cycle.

## 3. Results and Discussion

### 3.1. Characterization of $\text{Fe}_3\text{O}_4$ -PPE Catalyst

$\text{Fe}_3\text{O}_4$ -PPE catalyst was synthesized using reverse co-precipitation with ultrasonic wave flow (sonochemical method). The sonochemical method is reported to be able to assist the growth process of microscopic particles because the flow of ultrasonic waves can cause extreme conditions, where liquid bubbles grow and burst at very high temperatures and pressures at 5000 K and 20 Mpa, followed by very high cooling rates at 1010 K/s. This extreme condition is referred to as the phenomenon of acoustic cavitation [21].

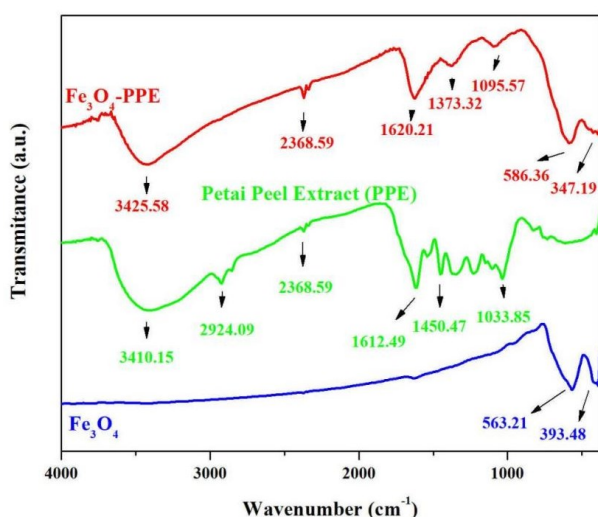


Figure 1. FTIR spectra of the  $\text{Fe}_3\text{O}_4$ -PPE catalyst

The performance of  $\text{Fe}_3\text{O}_4$ -PPE as a catalyst was affected by the presence of the  $\text{Fe}_3\text{O}_4$ -PPE active site [22]. FTIR was used to determine the type of functional group.  $\text{Fe}_3\text{O}_4$ -PPE has (the wavelength range is 340–4000 nm). Based on Figure 1, the functional groups of  $\text{Fe}_3\text{O}_4$ -PPE are the combination of the functional groups of petai peel extract and pure  $\text{Fe}_3\text{O}_4$ . The absorption shows the

presence of Fe-O bonds of  $\text{Fe}_3\text{O}_4$  at wavenumbers of 586.36  $\text{cm}^{-1}$  and 347.19  $\text{cm}^{-1}$  ( $\text{Fe}_3\text{O}_4$ -PPE) and 563.21 and 393.48  $\text{cm}^{-1}$  ( $\text{Fe}_3\text{O}_4$ ). The absorption in  $\text{Fe}_3\text{O}_4$ -PPE experienced a shift due to the interaction between the pure  $\text{Fe}_3\text{O}_4$  surface and the organic compounds in the petai peel extract. The Fe-O bonds are in tetrahedral and octahedral units. Fe-O bonds in octahedral units are indicated by absorption at 347.19  $\text{cm}^{-1}$ , while Fe-O bonds in tetrahedral units are indicated by absorption at 586.36  $\text{cm}^{-1}$  [18, 23, 24, 25].

The absorptions that appeared at 1033.85, 1450.47, 1612.49, 2924.09, and 3410.15  $\text{cm}^{-1}$  indicate the presence of functional groups of organic compounds derived from petai peel extracts, such as C-O stretching vibrations, C=C aromatic compounds,  $-\text{CH}_2$  stretching, and vibrations of the -OH groups of carboxylic acids, alcohols, and phenols [26, 27, 28, 29, 30]. Based on the FTIR spectra, the  $\text{Fe}_3\text{O}_4$ -PPE magnetic catalyst has been successfully synthesized using petai peel extract. However, an XRD analysis was needed to determine the type of iron oxide formed immiscible with other iron oxides, such as  $\text{Fe}_2\text{O}_3$ .

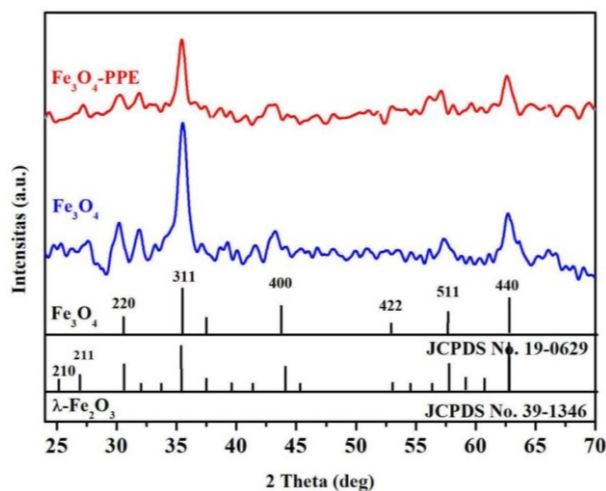


Figure 2. XRD diffractogram of  $\text{Fe}_3\text{O}_4$ -PPE catalyst

Based on Figure 2, the peaks on the  $\text{Fe}_3\text{O}_4$ -PPE and  $\text{Fe}_3\text{O}_4$  diffractograms appear at nearly the same  $2\theta$  (Miller index) values of 30° (220), 35° (311), 43° (400), 53° (422), 57° (511), and 62° (440). However, the peak intensity of  $\text{Fe}_3\text{O}_4$ -PPE is lower than that of  $\text{Fe}_3\text{O}_4$  due to the interaction of  $\text{Fe}_3\text{O}_4$  particles with organic compounds in the petai peel extract, which reduces crystallinity. The  $\text{Fe}_3\text{O}_4$ -PPE peaks are more identical to the characteristic peaks of  $\text{Fe}_3\text{O}_4$  (JCPDS No. 19-0629) than of  $\lambda\text{-Fe}_2\text{O}_3$  (JCPDS No. 39-1346), indicating that the magnetite ( $\text{Fe}_3\text{O}_4$ ) formed was not mixed with other iron oxides such as  $\lambda\text{-Fe}_2\text{O}_3$  (JCPDS No. 39-1346).

The magnetic properties of  $\text{Fe}_3\text{O}_4$ -PPE will enhance its catalytic performance.  $\text{Fe}_3\text{O}_4$  has stronger magnetic properties than  $\lambda\text{-Fe}_2\text{O}_3$ . The strong magnetic properties facilitate the separation process between the adsorbent and the filtrate using an external magnetic field for the reuse/regeneration of the catalyst. Based on the XRD diffractogram,  $\text{Fe}_3\text{O}_4$ -PPE crystal size information was determined using Debye-Scherrer's equation with full width at half maximum (FWHM = 0.461) of the (311) reflection. In this study, the  $\text{Fe}_3\text{O}_4$ -PPE crystal size

obtained was 8.41 nm. Compared to the results of previous studies (Table 3), the crystal size of Fe<sub>3</sub>O<sub>4</sub>-PPE is smaller, indicating improved crystallinity.

The results of the analysis using PSA are presented in Figure 3. There were three groups of particle size distribution from MPet, with percentages of 13.48%, 24.60%, and 74.02% for the 5.4 nm, 195 nm, and 2702.6 nm groups, respectively. Several sizes of magnetite particles from previous studies are presented in Table 3.

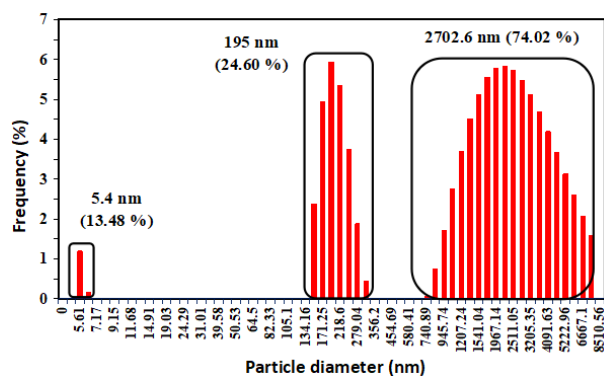


Figure 3. Particle size distribution of Fe<sub>3</sub>O<sub>4</sub>-PPE catalyst

Table 1. Comparison of crystal and particle sizes of Fe<sub>3</sub>O<sub>4</sub>

Extract source	Synthesis condition	Crystal size (nm)	Particle size (nm)	Morphology	Reference
Archidendron pauciflorum	Conventional method, 60 minutes, 60°C, FeSO <sub>4</sub> .7H <sub>2</sub> O, FeCl <sub>3</sub> .6H <sub>2</sub> O	17.6 and 20.9	318 and 294	-	[18]
	Room temperature, 30 minutes, FeCl <sub>3</sub>	-	10–100	rough surface	[31]
Hevea brasiliensis Muell. Arg. bark	Room temperature (27°C), 1 hour, FeCl <sub>3</sub> and FeCl <sub>2</sub>	-	200	-	[25]
Platanus orientalis	1 hour, 25°C Fe(NO <sub>3</sub> ) <sub>3</sub>	-	78–80 nm	rough surface	[32]
Parkia speciosa	Sonochemical method, 60 minutes, 60°C, FeSO <sub>4</sub> .7H <sub>2</sub> O, FeCl <sub>3</sub> .6H <sub>2</sub> O	8.41	5.4, 195, and 2702.6	-	This research

### 3.2. Biodiesel Synthesis using Fe<sub>3</sub>O<sub>4</sub>-PPE Catalyst

In this study, Fe<sub>3</sub>O<sub>4</sub>-PPE was applied as a catalyst in synthesizing biodiesel from WFO as a raw material. The WFO used in this study was sourced from household waste with a blackish-brown color. The performance of the Fe<sub>3</sub>O<sub>4</sub>-PPE catalyst in biodiesel production is presented in Figure 4. Based on Figure 4, using the Fe<sub>3</sub>O<sub>4</sub>-PPE catalyst

can reduce the % FFA of WFO by around 80%; the initial % FFA of WFO is 2.08%. This reduction is better when compared to the sulfuric acid catalyst, which is only about 50%. The Fe<sub>3</sub>O<sub>4</sub>-PPE catalyst plays a role in accelerating the transesterification of triglycerides and the esterification of free fatty acids (FFA) through their interactions with alcohols and the carbonyl groups of triglycerides and free fatty acids. The catalyst can increase the reaction rate between free fatty acids and alcohols during the same synthesis time.

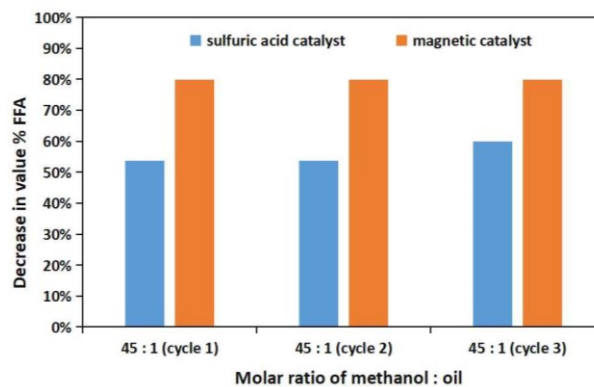


Figure 4. Performance of the Fe<sub>3</sub>O<sub>4</sub>-PPE catalyst for reducing the %FFA of WFO

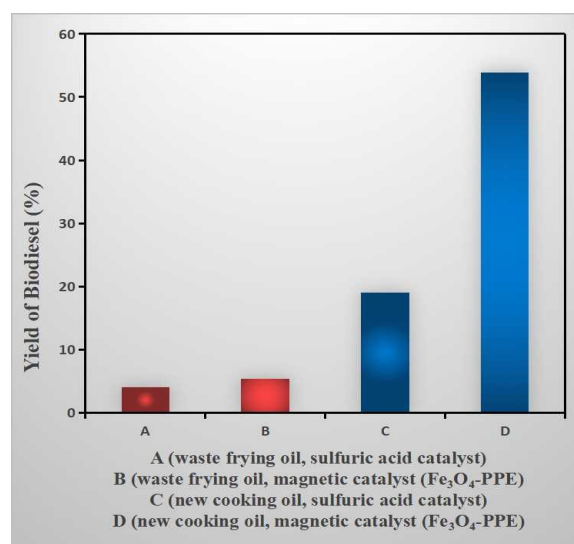


Figure 5. Performance of a Fe<sub>3</sub>O<sub>4</sub>-PPE catalyst for biodiesel production

Based on Figure 5, the yield of biodiesel produced using WFO with a Fe<sub>3</sub>O<sub>4</sub>-PPE catalyst is approximately 6%; this value is similar to the yield of biodiesel synthesized using WFO with a sulfuric acid catalyst, which is 4%. However, compared to the production of biodiesel from new cooking oil, the yield of biodiesel produced with Fe<sub>3</sub>O<sub>4</sub>-PPE catalyst is much higher, at 55%, compared to the sulfuric acid catalyst, which is at 18%. It means the performance of the Fe<sub>3</sub>O<sub>4</sub>-PPE catalyst is much better than the sulfuric acid catalyst to convert free fatty acids and triglycerides into biodiesel. The low biodiesel yield generated from WFO is due to the absence of triglycerides and free fatty acids in WFO. Allegedly, the repeated use with heating at high temperatures has destroyed the triglycerides and free fatty acids in WFO, making it unusable for biodiesel production. In addition,

impurities in WFO can prevent the transesterification and esterification reactions of triglycerides and free fatty acids into biodiesel. The yield produced from the new cooking oil raw material is also not optimal because the mass of the Fe<sub>3</sub>O<sub>4</sub>-PPE catalyst has not yet been optimized. Therefore, it is necessary for future research to optimize the mass of an enormous catalyst.

### 3.3. Characterization of the Synthesized Biodiesel Methyl Ester Using GC-MS

The primary fatty acid methyl esters in biodiesel cycles 1, 2, and 3 are presented in Tables 2, 3, and 4, respectively. In cycles 1, 2, and 3, the synthesized biodiesel has the same fatty acid content, although with slightly different percentages (Figure 6). The synthesized biodiesel's most extensive fatty acid is oleic and palmitoleic acids. From GC-MS analysis, it can be concluded that the Fe<sub>3</sub>O<sub>4</sub>-PPE catalyst can be used repeatedly in biodiesel synthesis without affecting the chemical properties of biodiesel.

**Table 2.** Main fatty acid methyl esters (FAME) in biodiesel from cycle 1 with Fe<sub>3</sub>O<sub>4</sub>-PPE catalyst

Peak	Area (%)	FAME	Common names for sources of fat
26.171	0.48	Pentadecanoic acid, 14-methyl-, methyl ester	Linoleic acid
31.145	1.17	Pentadecanoic acid, 14-methyl-, methyl ester	Linoleic acid
35.190	0.41	9-Hexadecenoic acid, methyl ester	Palmitoleic acid
35.809	43.39	9-Hexadecenoic acid, methyl ester	Palmitoleic acid
39.422	50.31	9-Octadecenoic acid, methyl ester	Oleic acid
39.754	1.12	Pentadecanoic acid, 14-methyl-, methyl ester	Linoleic acid
43.595	2.18	Oxiraneundecanoic acid, 3-pentyl-, methyl ester	-

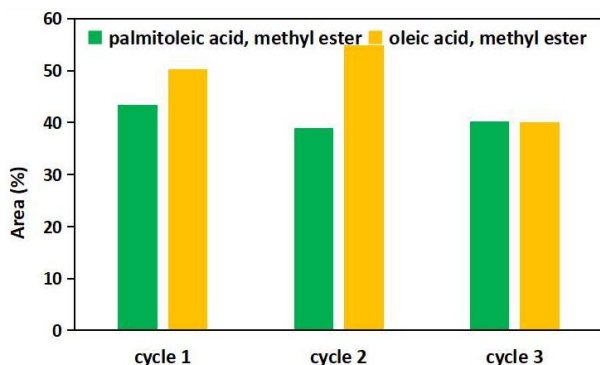


**Figure 6.** The main fatty acid methyl ester content of biodiesel produced three cycles with Fe<sub>3</sub>O<sub>4</sub>-PPE catalyst

**Table 3.** Main fatty acid methyl esters (FAME) in biodiesel from cycle 2 with Fe<sub>3</sub>O<sub>4</sub>-PPE catalyst

Peak	Area (%)	FAME	Common names for sources of fat
26.159	0.41	Pentadecanoic acid, 14-methyl-, methyl ester	Linoleic acid
31.133	1.04	Pentadecanoic acid, 14-methyl-, methyl ester	Linoleic acid
35.181	0.33	9-Hexadecenoic acid, methyl ester	Palmitoleic acid
35.742	38.97	Hexadecanoic acid, methyl ester	Palmitoleic acid
36.468	0.77	Octadecanoic acid	Oleic acid
39.128	11.49	9,12-Octadecadienoic acid, methyl ester	Oleic acid
39.345	43.31	11-Octadecenoic acid, methyl ester	Oleic acid
39.709	1.58	Octadecanoic acid, methyl ester	Oleic acid
40.016	0.90	9-Octadecenoic acid	Oleic acid

**Table 4.** Main fatty acid methyl esters (FAME) in biodiesel from cycle 3 with Fe<sub>3</sub>O<sub>4</sub>-PPE catalyst

Peak	Area (%)	FAME	Common names for sources of fat
26.151	0.41	Pentadecanoic acid, 14-methyl-, methyl ester	Linoleic acid
31.127	1.05	Pentadecanoic acid, 14-methyl-, methyl ester	Linoleic acid
35.170	0.33	9-Hexadecenoic acid, methyl ester	Palmitoleic acid
35.760	40.27	Hexadecanoic acid, methyl ester	Palmitoleic acid
36.483	0.65	Hexadecanoic acid, methyl ester	Palmitoleic acid
39.365	40.03	9-Octadecenoic acid, methyl ester	Oleic acid
39.714	1.32	Pentadecanoic acid, 14-methyl-, methyl ester	Linoleic acid
40.020	0.75	9-Octadecenoic acid, methyl ester	Oleic acid
43.506	2.33	Pentadecanoic acid, 14-methyl-, methyl ester	Linoleic acid

### 3.4. Testing the Quality of Biodiesel Products with Fe<sub>3</sub>O<sub>4</sub>-PPE as Catalyst

The quality of the synthesized biodiesel was tested using the parameters of density, moisture content, and acid number. This test was carried out in production cycles 1, 2, and 3. The test data is presented in Table 5. Based on Table 7, the densities of the synthesized biodiesel in cycles 1 and 2 were within the range of 850 to 890 kg/m<sup>3</sup>, which meets the SNI requirement. However,

the density of the produced biodiesel in cycle 3 exceeds the SNI standard. The acid values of biodiesel produced in cycles 1, 2, and 3 have met the SNI standard below 0.5 mg KOH/g. However, the water content values of biodiesel production in cycles 1, 2, and 3 are still above the SNI standard. Further treatment is needed to remove the water content of biodiesel.

Table 5. Data on biodiesel quality test results

Parameter	Units	SNI	Synthesized biodiesel		
			Cycle 1	Cycle 2	Cycle 3
Density	kg/m <sup>3</sup>	850–890	861	878	910
Water content	%	0.05	0.77	0.60	0.97
Acid number	mg KOH/g	<0.5	0.38	0.38	0.38

### 3.5. Reusability Studies of Fe<sub>3</sub>O<sub>4</sub>-PPE Catalyst

Fe<sub>3</sub>O<sub>4</sub>-PPE catalyst reusability studies on biodiesel production were carried out using the Fe<sub>3</sub>O<sub>4</sub>-PPE catalyst repeatedly in three production cycles. The biodiesel produced in each cycle was calculated for %FFA reduction, analyzed using GC-MS, and tested for biodiesel quality. The results showed no difference in reducing %FFA at three production cycles. Analysis using GC-MS showed that the methyl ester compounds of biodiesel produced in cycles 1, 2, and 3 were palmitoleic acid, methyl ester, and oleic acid, methyl ester. However, there is a slight difference in the percent abundance of biodiesel produced in cycle 3. The percentage abundances of palmitoleic acid, methyl ester, and oleic acid, methyl ester are, respectively, 43.39% and 50.31% for cycle 1, 38.97% and 43.31% for cycle 2, and 40.27% and 40.03% for cycle 3. The results of the biodiesel quality test, which included the acid number parameter, showed no significant difference between the biodiesel produced in cycles 1, 2, and 3. However, the density and water content parameters of biodiesel showed slight differences between the biodiesel produced in cycle 3 and those produced in cycles 1 and 2. From the study of the reusability of the Fe<sub>3</sub>O<sub>4</sub>-PPE catalyst in biodiesel production for three cycles, it can be concluded that the Fe<sub>3</sub>O<sub>4</sub>-PPE catalyst is reusable and can be used repeatedly in biodiesel production.

### 4. Conclusion

A reusable Fe<sub>3</sub>O<sub>4</sub>-PPE catalyst has been successfully synthesized using sonochemical methods. The crystal size of the MPet catalyst produced was 9.41 nm, while the particle size based on PSA consisted of three groups, i.e., 5.4 nm, 195 nm, and 2702.6 nm. The yield and reduction of % FFA of biodiesel produced from three production cycles using a reusable catalyst based on magnetic petai peels were similar, and there is no difference in the type of biodiesel methyl ester produced in three cycles; however, the biodiesel produced in cycle 3 has a slight difference in percent abundance. The results of the biodiesel quality test, which included the acid number parameter, showed no significant difference between the biodiesel produced in cycles 1, 2, and 3. However, the

density and water content parameters of biodiesel showed little difference between the biodiesel produced in cycle 3 and the biodiesel produced in cycles 1 and 2.

### Acknowledgment

The author would like to thank the Institute for Research and Community Service at UIN Sunan Kalijaga for the research funds given to the author. In addition, the authors also thank the UIN Sunan Kalijaga Integrated Laboratory for the facilities and infrastructure provided to complete this research.

### References

- [1] Maryam Helmi, Mahdi Ghadiri, Kambiz Tahvildari, Alireza Hemmati, Biodiesel synthesis using clinoptilolite-Fe<sub>3</sub>O<sub>4</sub>-based phosphomolybdic acid as a novel magnetic green catalyst from *salvia mirzayanii* oil via electrolysis method: Optimization study by Taguchi method, *Journal of Environmental Chemical Engineering*, 9, 5, (2021), 105988 <https://doi.org/10.1016/j.jece.2021.105988>
- [2] Bishwajit Changmai, Andrew E. H. Wheatley, Ruma Rano, Gopinath Halder, Manickam Selvaraj, Umer Rashid, Samuel Lalthazuala Rokhum, A magnetically separable acid-functionalized nanocatalyst for biodiesel production, *Fuel*, 305, (2021), 121576 <https://doi.org/10.1016/j.fuel.2021.121576>
- [3] Jefry Presson, Yohana Ivana Kedang, Maria Lilita Guterres, Risna Erni Yati Adu, Elisabeth Korbafo, Heri Suseno, Synthesis of Biodiesel from Feun Kase (*Thevetia peruviana*) Seed Oil Using NaOH Catalyst, *Jurnal Kimia Sains dan Aplikasi*, 25, 8, 270–279 <https://doi.org/10.14710/jksa.25.8.270-279>
- [4] Riza Habibi, Enny Fachriyah, Dewi Kusriani, Sintesis Biodiesel dari Minyak Mikroalga *Nannochloropsis* Sp. Melalui Transesterifikasi Menggunakan Katalis Basa, *Jurnal Kimia Sains dan Aplikasi*, 13, 1, (2009), 30–35 <https://doi.org/10.14710/jksa.13.1.30-35>
- [5] Newton A. Ihoeghian, Mohammed A. Usman, Exergetic evaluation of biodiesel production from rice bran oil using heterogeneous catalyst, *Journal of King Saud University-Engineering Sciences*, 32, 2, (2020), 101–107 <https://doi.org/10.1016/j.jksues.2018.11.007>
- [6] Sajad Tamjidi, Hossein Esmaeili, Bahareh Kamyab Moghadas, Performance of functionalized magnetic nanocatalysts and feedstocks on biodiesel production: a review study, *Journal of Cleaner Production*, 305, (2021), 127200 <https://doi.org/10.1016/j.jclepro.2021.127200>
- [7] Ali Bohlouli, Leila Mahdavian, Catalysts used in biodiesel production: a review, *Biofuels*, 12, 8, (2021), 885–898 <https://doi.org/10.1080/17597269.2018.1558836>
- [8] Isalmi Aziz, Edra Aditya Filipia Ardine, Nanda Saridewi, Lisa Adhani, Catalytic Cracking of Crude Biodiesel into Biohydrocarbon Using Natural Zeolite Impregnated Nickel Oxide Catalyst, *Jurnal Kimia Sains dan Aplikasi*, 24, 7, (2021), 222–227 <https://doi.org/10.14710/jksa.24.7.222-227>
- [9] Adeyinka S. Yusuff, Aman K. Bhonsle, Dinesh P. Bangwal, Neeraj Atray, Development of a barium-modified zeolite catalyst for biodiesel production from waste frying oil: Process optimization by

- design of experiment, *Renewable Energy*, 177, (2021), 1253–1264  
<https://doi.org/10.1016/j.renene.2021.06.039>
- [10] Maya Rahmayanti, Atika Yahdiyani, Ika Qurrotul Afifah, Eco-friendly synthesis of magnetite based on tea dregs ( $\text{Fe}_3\text{O}_4$ -TD) for methylene blue adsorbent from simulation waste, *Communications in Science and Technology*, 7, 2, (2022), 119–126  
<https://doi.org/10.21924/cst.7.2.2022.965>
- [11] Euripedes Garcia Silveira Junior, Oselys Rodriguez Justo, Victor Haber Perez, Inés Reyero, Ana Serrano-Lotina, Leonardo Campos Ramirez, Dayana F. dos Santos Dias, Extruded catalysts with magnetic properties for biodiesel production, *Advances in Materials Science and Engineering*, 2018, (2018), 3980967 <https://doi.org/10.1155/2018/3980967>
- [12] Indu Ambat, Varsha Srivastava, Esa Haapaniemi, Mika Sillanpää, Nano-magnetic potassium impregnated ceria as catalyst for the biodiesel production, *Renewable Energy*, 139, (2019), 1428–1436 <https://doi.org/10.1016/j.renene.2019.03.042>
- [13] Angelina Rianti, Elfa Karin Parassih, Agnes Erlinda Novenia, Alvin Christpoher, Devi Lestari, Warsono El Kiyat, Potensi Ekstrak Kulit Petai (*Parkia speciosa*) sebagai Sumber Antioksidan, *Jurnal Dunia Gizi*, 1, 1, (2018), 10–19 <https://doi.org/10.33085/jdg.v1i1.2901>
- [14] Yusof Kamisah, Faizah Othman, Hj Mohd Saad Qodriyah, Kamsiah Jaarin, *Parkia speciosa* hassk.: A potential phytomedicine, *Evidence-Based Complementary and Alternative Medicine*, 2013, (2013), 709028 <https://doi.org/10.1155/2013/709028>
- [15] Suchanuch Wonghirundecha, Soottawat Benjakul, Punnanee Sumpavapol, Total phenolic content, antioxidant and antimicrobial activities of stink bean (*Parkia speciosa* Hassk.) pod extracts, *Songklanakarin Journal of Science & Technology*, 36, 3, (2014), 301–308
- [16] Annisa Nurul Syakina, Maya Rahmayanti, Removal of methyl violet from aqueous solutions by green synthesized magnetite nanoparticles with *Parkia Speciosa* Hassk. peel extracts, *Chemical Data Collections*, 44, (2023), 101003  
<https://doi.org/10.1016/j.cdc.2023.101003>
- [17] Maya Rahmayanti, Sri Juari Santosa, Sutarno Sutarno, Comparative Study on the Adsorption of  $[\text{AuCl}_4]^-$  onto Salicylic Acid and Gallic Acid Modified Magnetite Particles, *Indonesian Journal of Chemistry*, 16, 3, (2016), 329–337  
<https://doi.org/10.22146/ijc.21150>
- [18] Maya Rahmayanti, Annisa Nurul Syakina, Is Fatimah, Triastuti Sulistyaningsih, Green synthesis of magnetite nanoparticles using peel extract of jengkol (*Archidendron pauciflorum*) for methylene blue adsorption from aqueous media, *Chemical Physics Letters*, 803, (2022), 139834  
<https://doi.org/10.1016/j.cplett.2022.139834>
- [19] Maya Rahmayanti, Guliston Abdillah, Sri Juari Santosa, Sutarno Sutarno, Application of Humic Acid Isolated From Kalimantan Peat Soil Modifying Magnetite for Recovery of Gold, *Jurnal Bahan Alam Terbarukan*, 8, 2, (2020), 77–83  
<https://doi.org/10.15294/jbat.v8i2.20392>
- [20] Maya Rahmayanti, Sri Juari Santosa, Sutarno Sutarno, Modified Humic Acid from Peat Soils with Magnetite ( $\text{Ha-Fe}_3\text{O}_4$ ) by Using Sonochemical Technology for Gold Recovery, *Jurnal Bahan Alam Terbarukan*, 9, 2, (2020), 81–87  
<https://doi.org/10.15294/jbat.v9i02.26131>
- [21] Maya Rahmayanti, Sri Juari Santosa, Sutarno Sutarno, Sonochemical co-precipitation synthesis of gallic acid-modified magnetite, *Advanced Materials Research*, 1101, (2015), 286–289  
<https://doi.org/10.4028/www.scientific.net/AMR.1101.286>
- [22] Yi-Tong Wang, Zhen Fang, Xing-Xia Yang, Ya-Ting Yang, Jia Luo, Kun Xu, Gui-Rong Bao, One-step production of biodiesel from *Jatropha* oils with high acid value at low temperature by magnetic acid-base amphoteric nanoparticles, *Chemical Engineering Journal*, 348, (2018), 929–939  
<https://doi.org/10.1016/j.cej.2018.05.039>
- [23] Yen Pin Yew, Kamyar Shameli, Mikio Miyake, Noriyuki Kuwano, Nurul Bahiyah Bt Ahmad Khairudin, Shaza Eva Bt Mohamad, Kar Xin Lee, Green synthesis of magnetite ( $\text{Fe}_3\text{O}_4$ ) nanoparticles using seaweed (*Kappaphycus alvarezii*) extract, *Nanoscale Research Letters*, 11, (2016), 276  
<https://doi.org/10.1186/s11671-016-1498-2>
- [24] Hassan Rasoulzadeh, Anoushiravan Mohseni-Bandpei, Mehdi Hosseini, Mahdi Safari, Mechanistic investigation of ciprofloxacin recovery by magnetite-imprinted chitosan nanocomposite: isotherm, kinetic, thermodynamic and reusability studies, *International Journal of Biological Macromolecules*, 133, (2019), 712–721  
<https://doi.org/10.1016/j.ijbiomac.2019.04.139>
- [25] Abin Sebastian, Ashwini Nangia, M. N. V. Prasad, Cadmium and sodium adsorption properties of magnetite nanoparticles synthesized from *Hevea brasiliensis* Muell. Arg. bark: Relevance in amelioration of metal stress in rice, *Journal of Hazardous Materials*, 371, (2019), 261–272  
<https://doi.org/10.1016/j.jhazmat.2019.03.021>
- [26] Denga Ramutshatsha-Makhwedzha, Avhafunani Mavhungu, Mapula Lucey Moropeng, Richard Mbaya, Activated carbon derived from waste orange and lemon peels for the adsorption of methyl orange and methylene blue dyes from wastewater, *Heliyon*, 8, 8, (2022), e09930  
<https://doi.org/10.1016/j.heliyon.2022.e09930>
- [27] Cristiele Costa de Souza, Lorrana Zélia Martins de Souza, Murat Yilmaz, Magno André de Oliveira, Augusto Cesar da Silva Bezerra, Edilaine Ferreira da Silva, Marcello Rosa Dumont, Alan Rodrigues Teixeira Machado, Activated carbon of *Coriandrum sativum* for adsorption of methylene blue: Equilibrium and kinetic modeling, *Cleaner Materials*, 3, (2022), 100052  
<https://doi.org/10.1016/j.clema.2022.100052>
- [28] P. C. Nnaji, V. C. Anadebe, I. G. Ezemagu, O. D. Onukwuli, Potential of *Luffa cylindrica* seed as coagulation-flocculation (CF) agent for the treatment of dye wastewater: Kinetic, mass transfer, optimization and CF adsorption studies, *Arabian Journal of Chemistry*, 15, 2, (2022), 103629  
<https://doi.org/10.1016/j.arabjc.2021.103629>
- [29] Maya Rahmayanti, Erni Yunita, Nunung Faizah Yosi Putri, Study of adsorption-desorption on batik industrial dyes (naphthol blue black) on magnetite modified humic acid ( $\text{HA-Fe}_3\text{O}_4$ ), *Jurnal Kimia Sains*

dan Aplikasi, 23, 7, (2020), 244-248  
<https://doi.org/10.14710/jksa.23.7.244-248>

- [30] Maya Rahmayanti, Indah Nurhikmah, Feni Larasati, Isolation, Characterization and Application of Humin From Sumatran Peat Soils as Adsorbent for Naphtol Blue Black and Indigosol Blue Dyes, *Molekul*, 16, 1, (2021), 67-74  
<http://dx.doi.org/10.20884/1.jm.2021.16.1.700>
- [31] Abin Sebastian, Ashwini Nangia, M. N. V. Prasad, A green synthetic route to phenolics fabricated magnetite nanoparticles from coconut husk extract: implications to treat metal contaminated water and heavy metal stress in *Oryza sativa* L., *Journal of Cleaner Production*, 174, (2018), 355-366  
<https://doi.org/10.1016/j.jclepro.2017.10.343>
- [32] Henam Sylvia Devi, Muzaffar Ahmad Boda, Mohammad Ashraf Shah, Shazia Parveen, Abdul Hamid Wani, Green synthesis of iron oxide nanoparticles using *Platanus orientalis* leaf extract for antifungal activity, *Green Processing and Synthesis*, 8, 1, (2019), 38-45  
<https://doi.org/10.1515/gps-2017-0145>